

# Graphite Presentation to USNRC in support of PBMR Pre-application Activities

## Supporting Document

Mark Davies  
October 9, 2001

### **Pebble Bed Modular Core Structures Design**

The PBMR core structures consist of a graphite reflector supported and surrounded by a metallic core barrel. They are housed within the Reactor unit of the Main Power System.

The metallic core barrel bears and supports the graphite reflector and acts a gas baffle separating the main gas flow from the reactor pressure vessel. SS 316 has been chosen as the core barrel material.

The graphite reflector consists of a substantial number of blocks arranged in circular rings of discrete columns. The graphite reflector can be sub-divided into three sub-systems, namely the bottom, side and top reflector.

The PBMR core structures are designed to maintain the following safety functionality requirements

- Pebble Bed Geometry
- Adequate Cooling of the Pebble Bed
- Access for the Reactivity Control and Shutdown Systems
- De-fuelling Route

### **Pebble Bed Geometry**

The reactor core cavity is formed by the side reflector and the bottom reflector. The side reflector is supported in the region of the pebble bed by circumferential restraints, which are not attached to the core barrel. The side reflector is split into an inner replaceable side reflector and an outer permanent side reflector.

Due to the inherent variability of the coefficient of thermal expansion of graphite and the substantial height of the reactor, the side reflector is arranged in discrete columns.

The bottom reflector is supported from the metallic base plate and designed so that the top blocks form a 30-degree cone.

The top reflector is suspended from the core barrel top plate by means of carbon-carbon composite tie rods.

I-17

The reactor core cavity is filled with approximately 430,000 spheres approximately 60 mm in diameter. Some 100,000 of these spheres are graphite spheres and occupy the central zone of the pebble bed (approximately 25% of the cross sectional area). The remaining 330,000 spheres are fuel spheres arranged in an annulus around the central graphite region. The pebble bed is maintained in this configuration by recirculating spheres throughout the life of the reactor. This is achieved by defuelling from the bottom of the pebble bed, checking for spent fuel and recirculating to the top of the pebble bed. The fuel is recirculated using a pneumatic helium transfer system. There are 9 recirculating fuel pipes arranged around the periphery of the top reflector and 1 graphite-recirculating pipe in the centre of the top reflector.

### **Adequate Cooling of the Pebble Bed**

The coolant paths are a mixture of radiation, conduction and convection, either forced or natural. The core structures are required to ensure that these cooling paths are sufficient under all operating conditions to ensure that the limiting temperatures of the fuel are not exceeded. In normal operation the peak fuel temperature is limited to 1300 deg C. In upset condition the peak fuel temperature is limited to 1600 deg C.

The core structures are designed to achieve the above fuel temperature limits without active systems. This is achieved by the design of a core barrel with a large surface area to volume ratio (long narrow cylinder). Under a Pressurised Loss Of Forced Cooling (PLOFC) condition care must be taken in the design to ensure that the core barrel does exceed temperature limits due to natural circulation of hot gas from the core.

The main flow paths within the core structures are as follows:

The inlet coolant returning to the core from the recuperator is directed into a lower plenum beneath the core base plate. The lower plenum is formed as part of the core support structure and redirects flow to the annulus formed between the side reflector and the core barrel. The lower plenum achieves a uniform distribution of mass flow around the annulus with minimal impact on circuit pressure losses.

The gas flows up the annulus and enters the pebble bed near the top of the side reflector. Leakage into the core is minimised by a series of vertical graphite keys in both the inner and outer side reflector blocks. These keys effectively form two dams and create three pressure zones, the annulus between the side reflector and the core barrel (highest pressure), the annulus between the inner and outer rings of keys and the pebble bed (lowest pressure).

The gas then flows down through the pebble bed and exits the pebble bed through slots between the columns of bottom reflector blocks. Due to the annular design of the core approximately 20-25% of the gas flows through the graphite region and does not receive nuclear heating (other than some gamma heating from the graphite) and exits the core at a relatively low temperature. The remainder of the gas flows through the fuelled region and exits the core at a high temperature. This leads to a stratification of the gas and temperature gradients in the bottom reflector blocks.

The outlet plenum is designed to generate swirl and induce mixing to reduce the temperature stratification within the gas prior to the hot gas duct upstream of the high pressure, turbo

compressor. The PBMR design is based on earlier German designs and the differential temperature within the gas leaving the core is less than 60 deg C.

There is a channel from the outlet plenum to the hot gas duct through the side reflector. To minimise pressure losses and gas velocities the channel should be as large as possible. However this is limited by maximum block sizes available from graphite manufacturers. This channel is connected to the hot gas duct via a seal, which is located on the core barrel.

### **Access for Reactivity Control Shutdown System RCSS**

The design of the core neutronics is such that the reactor can be shutdown solely through insertion of absorbers into the side reflector columns. Independent and diverse shutdown systems are provided, the control rod system and the small absorber sphere system.

The position of the RCSS within the side reflector has been determined to be approximately 60 mm from the front face. All RCSS channels are sleeved to minimise flow leakage and the sleeves are the primary safety feature of the core structures with regard to maintaining access for the RCSS. This geometry requirement has a significant impact on the structural performance of the blocks during the lifetime of the plant.

### **Defuelling Route**

The shape and structure of the side reflector and bottom reflector are designed to ensure smooth pebble flow into the Defuelling chute. The Defuelling chute is constructed from courses of graphite rings supported and centred on the metallic base plate. The inner ring of top blocks extending over the defuelling chute rings achieves a smooth transition from the top of the bottom reflector into the defuelling chute.

The top blocks of the bottom reflector that form the 30 degree cone are stepped vertically between adjacent rings to accommodate any potential column to column variation in CTE. This step ensures a gradient from the outside of the pebble bed to the Defuelling chute under all operating conditions.

### **Reactor Temperatures and Fluences**

The following table gives the distribution of temperature and fluence for various axial positions and three radial positions 1) inside of inner side reflector 2) interface between inner and outer side reflector columns and 3) outside of outer side reflector column.

The peak fluence of approximately  $165 \cdot 10^{20}$  n/cm<sup>2</sup> EDN (equivalent dido nickel) occurs at a temperature of between 720 °C and 800 °C. This is an onerous irradiation requirement for graphite.

PBMR Reactor Data							
	Temperature °C				Fluence EDN n/cm <sup>2</sup>		
Axial Position cm	Radial Position				Radial Position		
	185 cm	225 cm	275 cm		185 cm	225 cm	275 cm
0	4.96E+02	4.96E+02	4.98E+02		5.06E+20	8.98E+18	3.28E+16
70	5.01E+02	4.97E+02	4.98E+02		2.70E+21	6.02E+19	3.32E+17
150	5.12E+02	4.97E+02	4.98E+02		7.26E+21	1.73E+20	1.04E+18
230	5.76E+02	4.98E+02	4.99E+02		1.03E+22	2.45E+20	1.48E+18
310	6.40E+02	4.99E+02	4.99E+02		1.35E+22	3.21E+20	1.94E+18
390	7.20E+02	5.00E+02	4.99E+02		1.60E+22	3.78E+20	2.28E+18
470	8.01E+02	5.01E+02	4.99E+02		1.59E+22	3.79E+20	2.29E+18
550	8.74E+02	5.02E+02	4.99E+02		1.43E+22	3.40E+20	2.06E+18
630	9.37E+02	5.03E+02	4.99E+02		1.20E+22	2.87E+20	1.73E+18
710	9.89E+02	5.04E+02	5.00E+02		9.10E+21	2.17E+20	1.31E+18
790	1.03E+03	5.05E+02	5.00E+02		7.42E+21	1.77E+20	1.07E+18
870	1.07E+03	5.07E+02	5.00E+02		5.13E+21	1.22E+20	7.35E+17
955	9.80E+02	5.07E+02	5.00E+02		2.59E+21	5.84E+19	3.54E+17

Note: the 0 cm axial point refers to a position just below the top reflector.

## Graphite

### Nuclear Graphite Manufacture

Graphites are manufactured for a wide variety of applications. Nuclear applications of graphite have been around for over half a century since the first chain reaction in the Chicago Pile in 1942. Since then over one hundred graphite-moderated reactors have been constructed and safely operated for a number of years. Many are still operating today.

Generally the requirements for nuclear grade graphite can be summarised by the following:

- Low neutron capture cross section
- High purity
- Dimensional stability when subjected to irradiation
- Good mechanical properties
- High density
- Good isotropy
- Homogeneous structure
- Large dimensions

There are a number of raw material and process variables that can be combined to produce graphites with wide ranging properties. The raw materials include coke source, binder and impregnation materials. The process variables include particle size, fabrication technique and purification.

The particle size variation is generally classified into coarse, medium and fine grain material. Typically, medium grain graphites have been used for nuclear applications in the UK, Germany and the US. More recently fine grain materials have been used for the HTTR in Japan and the HTR-10 in China.

Currently there is considerable debate in the graphite community over which material represents the best option for use as a moderator material in high temperature reactors. Generally, when compared with medium grain graphite, fine grain graphite has better dimensional stability and lower material property changes when subjected to irradiation. However fracture properties of fine grain materials are considered to be inferior due to the more homogeneous nature of its structure compare to medium grain.

Graphite is manufactured in a number of stages

- Raw materials – assembly of coke, pitch etc
- Milling – grinding coke particles to required size
- Mixing – combining ground particle with pitch to - plastic mass
- Fabrication – moulding or extruding – green article
- Baking – 850 - 1200 deg C for 30 - 70 days – carbon artefacts
- Impregnation – density recovery by re-impregnation with pitch
- Graphitisation – 2800 – 3200 deg C for 15 days
- Purification

The impregnation and baking stages can be repeated to improve mechanical strength and density. Graphitisation for nuclear materials is generally done in an Acheson furnace with direct pyrometric measurements for temperature control within the furnace.

The fabrication process generally falls into three basic processes, extrusion, isostatic moulding and vibration moulding.

Extrusion tends to yield graphites that are less isotropic and less dimensionally stable than moulded graphites. Moulded graphites tend to be available in smaller dimensions than extruded graphites although vibration moulding can produce substantial block sizes as well. However moulded graphites are substantially more expensive than extruded graphites.

## **Material Properties**

### Unirradiated Data

A wide range of materials can be produced by manufacturers ranging from pitch or petroleum coke through medium or fine grain to extruded or vibration moulded. PBMR has chosen Sigr Great Lakes, SGL as the preferred supplier for the graphite reflector. The range of products available to the PBMR design team are shown in the Table below.

Property	Sleeve	Grade 1	Grade 2	Iso	Sasol
Density ( $10^3 \text{Kg/m}^3$ )	1.79	1.75	1.79	1.82	1.79
Thermal Conductivity (W/m.K)		130	130	133	130
CTE 20-200 °C ( $10^{-6}/\text{K}$ )	4.35	4.2	4.4	4.1	4.7
Neutron Absorbancy (mBarns)	4.62	4.5	5.4	4.0	12
Compressive Strength (MPa)	72	55	65	100	70
Modulus of Elasticity (GPa)	8.9	9	10	10	10
Poisson's Ratio	0.21	0.21	0.21	0.21	0.21
Anisotropy Ratio (Par/Per)	1.1	1.1	1.1	1.1	1.1

### SGL Graphite Material Database

The properties above are for unirradiated material and all have broadly similar properties except for the iso and sasol material. The iso material has a higher strength and the sasol coke shown is produced locally in South Africa as a by-product of the coal to oil process employed by SASOL pty Ltd. It has a high Boron content and therefore is unlikely to be used adjacent to the pebble bed but could be used in the permanent reflector.

### Irradiated Behaviour

In order to understand the irradiation behaviour of polycrystalline nuclear graphite, it is essential to understand the behaviour of the graphite crystallites that are the main structural component of nuclear graphite. The structure of polycrystalline graphite is usually described using several terms that require explanation.

#### Crystallite (or crystal)

This is the structure of carbon atoms, which defines its periodic array, see Figure 1. The 'a' spacing has been determined to be  $2.4612 \pm 0.0001 \text{ \AA}$  and the 'c' spacing, which encompasses two basal planes, as  $6.7079 \pm 0.0007 \text{ \AA}$ . The unit cell contains four atoms and has a volume of  $35.190 \text{ \AA}^3$ . Crystal density is  $2.266 \text{ g/cm}^3$ . The interlayer spacing is usually referred to by the symbol 'd' and is equal to half of 'c'.

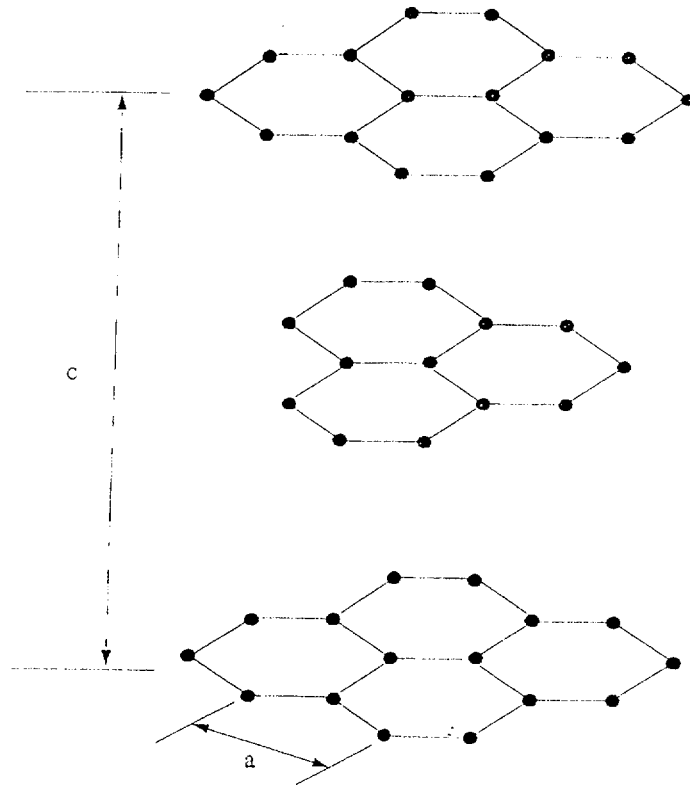


Figure 1. The Graphite Crystal Lattice

### Crystallite size

This is the apparent size of a crystallite as measured using X-ray diffraction methods. It is usually quoted as ' $L_a$ ' and ' $L_c$ ', that is the mean layer diameter (measured in the ' $a$ ' direction) and the average thickness (measured in the ' $c$ ' direction). Values of 435 Å and 600 Å to 400 Å for ' $L_a$ ' and ' $L_c$ ' respectively have been quoted for Pile Grade A, PGA graphite used in the MAGNOX reactors in the UK. However other references give widely different estimates.

### Mrozowski cracks

When the graphite crystallites cool from the graphitisation temperature, cracks are formed due to the large difference in the coefficient of expansion in the ' $a$ ' and ' $c$ ' direction. It has been calculated by Mrozowski that these cracks can lead to some 7- 8.4% porosity in the crystallite reducing the theoretical density to  $\sim 2.0$  from  $\sim 2.26 \text{ g/cm}^3$ .

### Coke particle (or Grain)

These are discrete coke particles and in the green condition, "before calcining and baking", range from less than 0.074 mm up to 6 mm in size. The coke particles in Gilsocarbon graphite (used as the moderator in the AGR programme in the UK) are particularly interesting as the crystallites are arranged into spherical grains with the basal plane lying perpendicular to the radial direction. It is this quality, along with the moulding process, that leads to the isotropic nature of Gilsocarbon graphites. Unfortunately this graphite is no longer available.

By contrast most coke grains are more lenticular and in the extreme may be needle like. On extrusion of the graphite billets, or “green article”, the lenticular shape of these particles may lead to the anisotropic material properties in the final product. This may be desirable in some graphite products, however for stable nuclear graphites a product with as near isotropic properties is desired. All of the graphites in the Table above have anisotropy ratios as defined by measurements of the Coefficient of Thermal Expansion (CTE) in different directions of ~1.1. An extreme example of early anisotropic nuclear graphites with isotropy ratios in the region of 2 as used in the nuclear industry, would be PGA and GR-280, as used in the Magnox and RBMK reactors respectively.

Calcined coke particle (or grain)

In the calcined state the coke particles are fused into the main carbon body. The coke particles shrink and form regions in which the crystallites are highly aligned, surrounded by unaligned binder. In nuclear graphites, a typical grain size is ~0.02 to 1mm. The grain size is an important factor to be taken into account when considering fracture of polycrystalline graphite.

Pores

Voids between crystallites and other particles are referred to as pores. They can vary in size from ~10 Å to many microns in size. In the unirradiated state, some of this porosity is accessible to the surrounding gas whilst the other is closed. Gilsocarbon has an open pore volume of ~0.11 cm<sup>3</sup>/cm<sup>3</sup> and a closed pore volume of 0.086 cm<sup>3</sup>/cm<sup>3</sup>.

## The Damage Process

Typical polycrystalline graphite consists of about 80% pitch coke and 20% binder. When graphite is irradiated, the changes in material properties are a primary function of irradiation damage to the graphite crystallites. In trying to understand irradiation damage in the polycrystalline form, it is therefore necessary, to understand the crystal damage process; in particular, the effect of temperature is important. A short description of irradiation damage in graphite crystallites is given below. This is later referenced to the polycrystalline material property changes.

Fast neutron energies in a thermal reactor generally range from less than 1eV to ~10MeV with a mean energy of ~2MeV. Radiation damage occurs in graphite when used as a moderator, due to carbon atoms being displaced from the crystal lattice. Billiard ball mechanics can be used to estimate the energy required to displace a carbon atom. Models based on this concept can be used to define a damage function to relate the fast neutron flux to the irradiation damage.

A model used to assess the damage caused by fast neutrons is based on the displacement rate of atoms within the lattice. For atoms irradiated in a neutron flux between  $E_n$  and  $E_n + dE_n$  the displacement rate,  $dN/dt$ , can be defined as:

$$\frac{dN}{dt} = \int \phi(E_n) \sigma(E_n) \bar{v}(E_n) dE_n \quad \text{atoms / atom / s}$$

Where  $\phi(E_n)$  is the flux,  $\sigma(E_n)$  is the capture cross-section for carbon atoms and  $\bar{\nu}(E_n)$  is the average number of displacements produced by collisions of energy  $E_n$ .

Various versions of the damage function  $\bar{\nu}(E_n)$  have been devised. More recent versions not only include energy losses due to primary and secondary knock-ons, but also losses due to electronic processes.

Work in the UK (principally Simmons) and elsewhere has shown that at high energies the probability of damage is greater and that the energy transfer from a primary knock-on is only a small fraction of the initial energy of the moving atom. At lower energies there is a tendency towards an equal distribution between the moving and struck atoms.

It has also been showed that for the primary knock-ons, at high energies, the mean distance between displacement collisions was large compared with the graphite lattice inter-atomic spacing. The secondary knock-on energy is less than 500eV; at this energy, the mean distance between collisions becomes comparable to the lattice spacing. From this work it is therefore predicted that a primary knock-on would produce separate groups of secondary knock-ons as illustrated in Figure 2.

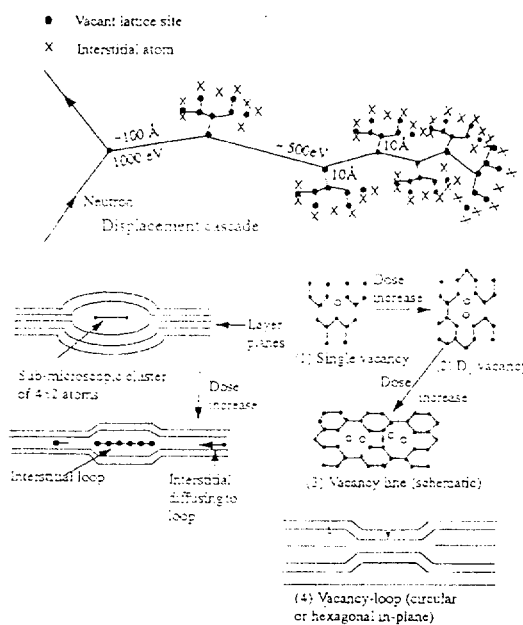


Figure 2. Graphite Damage Mechanism (after Simmons[4]).

Displaced carbon atoms recombine into vacant positions within the graphite crystal lattice, are lost to the boundaries, or combine with other atoms to form interstitial loops in the relatively large inter-layer spacing. Likewise vacant sites may eventually join together to form small vacancy loops, which may eventually lead to collapse of the basal planes.

The formation of and movement of interstitial and vacancy groups was studied extensively in the early 1960s. Interstitial atoms were found to be mobile even at low temperatures and will combine to form small groups. Between 150°C and 650°C these groups grow in size (and

reduce in number) with increasing temperature, but tend to become less mobile the larger the group. Vacancies do not start to be mobile until irradiation temperatures of  $\sim 650^{\circ}\text{C}$  are reached.

### Crystal Dimensional Changes

Crystal dimensional changes have been studied in the UK using Pyrolytic graphite -see Figure 3. The expansion in the 'c' direction can be explained by the presence of interstitial atoms between the graphite lattice planes. The contraction in the 'a' direction is more difficult to explain. Mechanisms that have been proposed for the shrinkage in the 'a' direction are:

- i. Elastic relaxation around vacant sites
- ii. Poisson's ratio effect accompanying the 'c' expansion
- iii. Buckling of the lattice by interstitial clusters
- iv. Modification of the inter-atomic linkage due to the presence of the vacancies

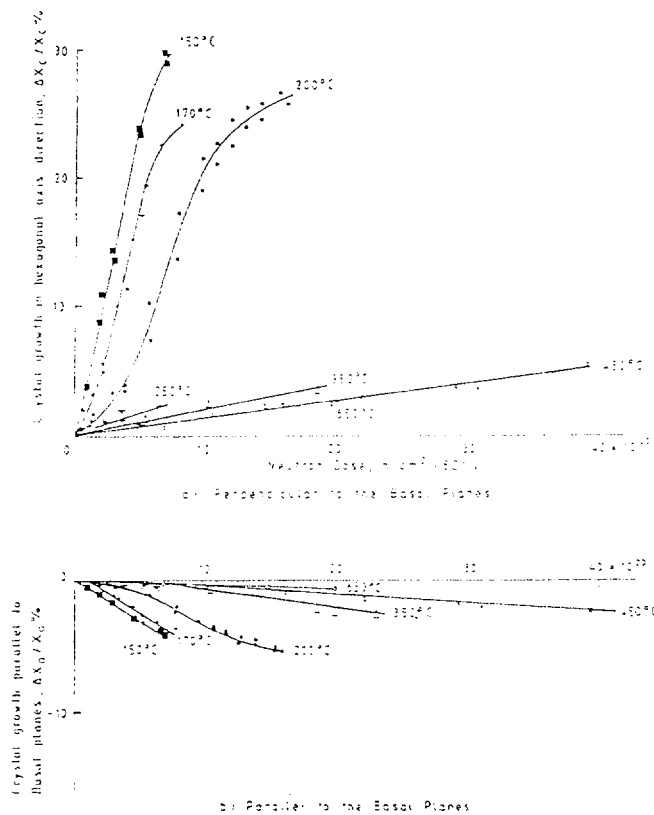


Figure 3. Crystal Dimensional Changes (after Kelly[6])

The experimental data given in Figure 3 show that the largest dimensional changes occur at low temperatures, below  $300^{\circ}\text{C}$ , fortunately this temperature range is of no interest to the PBMR. However at higher irradiation temperatures, above  $\sim 750^{\circ}\text{C}$ , there appears to be an increase in dimensional change rate which is dependent on the crystal size. In addition in this temperature range there is an increase in the creep rate around this temperature. Both these effects may be responsible for the sudden change in shrinkage behaviour in polycrystalline graphite that occurs between 800 and  $1100^{\circ}\text{C}$ .

## Crystal Coefficient of Thermal Expansion (CTE)

In determining CTE, the dimensional change of the crystallite must also be considered along with its irradiation changes in the CTE.

The CTE of a graphite crystal is much larger in the 'c' direction than in the 'a' direction. For example the instantaneous value of CTE at 70°C is  $\sim 26.5 \times 10^{-6} \text{ K}^{-1}$  in the 'c' direction and  $\sim -1 \times 10^{-6} \text{ K}^{-1}$  in the 'a' direction. Many authors have studied the temperature dependence of polycrystalline graphites CTE on the individual crystallite CTE. Use is made of this dependence to convert CTE from one range to another range. It is interesting to note the instantaneous CTE of the crystallite in the 'a' direction is zero at 400°C.

When subjected to fast neutron irradiation at relatively low temperatures, below  $\sim 250^\circ\text{C}$ , the CTE in the 'c' direction reduces at a dose of  $\sim 5 \times 10^{20} \text{ n/cm}^2$ , whilst at a similar dose the CTE in the 'a' direction increases from a small negative value to a small positive value, see Figure 4. This behaviour appears to be associated with the large growth in the 'c' axis at these lower irradiation temperatures. Fortunately this complication is not of interest in the PBMR since the inlet temperature of PBMR is in excess of  $500^\circ\text{C}$ .

At higher irradiation temperatures, above  $\sim 300^\circ\text{C}$ , the CTE of the crystallite in both the 'a' and 'c' appears to be independent of irradiation dose, remaining at the unirradiated value, however data to confirm this finding only exist for  $\sim 450$  and  $600^\circ\text{C}$ .

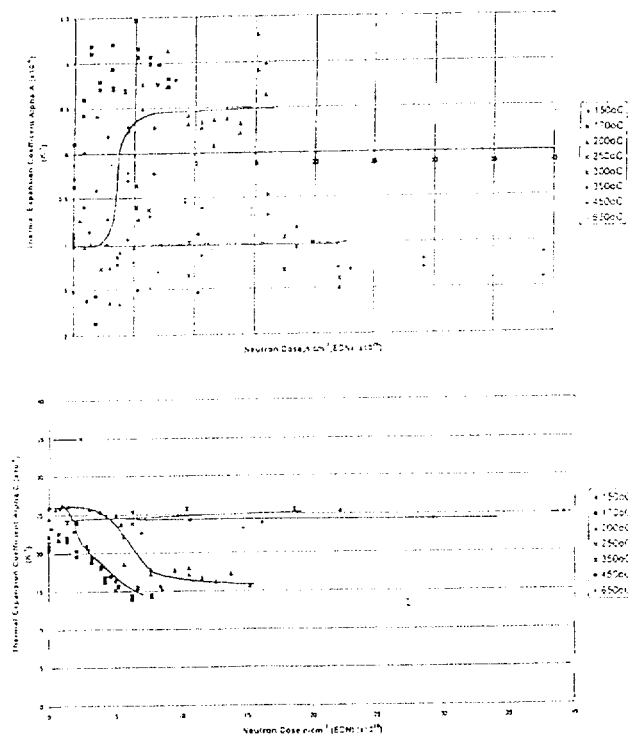


Figure 4. Change in Graphite CTE with Irradiation

## Crystal Mechanical Properties

### Elastic Constants for a Perfect Crystal

Elastic Modulus (N/m <sup>2</sup> x 10 <sup>10</sup> )		Elastic Compliance (m <sup>2</sup> /N x 10 <sup>-12</sup> )	
$C_{11}$	106	$S_{11}$	0.98
$C_{12}$	18	$S_{12}$	-0.16
$C_{13}$	1.5	$S_{13}$	-0.33
$C_{33}$	3.46	$S_{33}$	27.5
$C_{44}$	0.45	$S_{44}$	0.24

As would be expected by consideration of the structure of the crystal lattice, the modulus parallel to the basal plane ( $C_{11}$ ) is much larger than perpendicular to the basal plane ( $C_{33}$ ). The shear modulus parallel to the basal plane ( $C_{44}$ ) is relatively low, but the shear modulus for a single layer is higher as:

$$G = \frac{1}{2}(C_{11} - C_{12}) = 44 \times 10^{10} \text{ N / m}^2$$

With irradiation  $C_{33}$  tends to slightly reduce whilst  $C_{44}$  significantly increases. Both these elastic moduli are associated with inter-layer forces. The decrease in  $C_{33}$  can be explained by the large increase in inter-layer spacing at low temperatures, whilst the increase in  $C_{44}$  has been associated with pinning of glissile dislocations associated with the basal plane.

### Crystal Thermal Conductivity

The changes to thermal conductivity with irradiation are large and are dependent on the irradiation temperature. The graphite crystal possesses two principal conductivities,  $K_c$  and  $K_a$ , measured parallel and perpendicular to the hexagonal axis. Measurements have shown that  $K_a \gg K_c$ .

In the temperature ranges of interest in the PBMR, lattice vibrations dominate the thermal conductivity of a graphite crystal. At high temperatures, phonon scattering controls the conductivity of the crystal, both perpendicular and parallel to the basal plane. Increasing temperature increases phonon scattering. In a less than perfect crystal, scattering will occur at defects and the effect of irradiation will increase the number of defects within the lattice, thus reducing the thermal conductivity. In polycrystalline graphites, the thermal conductivity is much less than  $K_c$ .

### Equivalent Fluence and Temperature

The fast neutron flux spectrum differs from reactor to reactor. The displacement rate, and thus, the damage to graphite is dependent on the flux spectrum. Thus, it is necessary to equate graphite damage to a standard position/flux spectrum.

The units of fluence that are likely to be of interest to PBMR are displacements per atom, Equivalent DIDO Nickel (EDN) and integrated fluence for energies greater than 0.18 MeV.

$$\begin{aligned} 1.0\text{n/cm}^2 \text{ EDND} &\equiv 1.5 \text{ n/cm}^2 (E_d > 0.18 \text{ MeV}) \\ 7.62\text{n/cm}^2 \text{ EDND} &\equiv 1 \text{ dpa} \end{aligned}$$

The Equivalent Temperature concept is controversial and has only been used to any extent in the UK. It was developed in the UK in the 1950s to explain the differences in the irradiated properties of graphite specimens irradiated at the same temperature but at different fluxes in different reactors. The reasoning behind the concept is as follows:

Fast neutron damage to graphite is not only a function of irradiation dose and temperature, but is also a function of time. For example if similar graphite samples were irradiated at the same temperature, to the same irradiation dose in two different times, the one which reached the dose in the faster time would exhibit more irradiation damage than the other. This is because the sample that was irradiated for the longer period would have had time for more irradiation annealing to take place.

There are several problems associated with the use of an equivalent temperature concept as currently defined. These are listed below:

1. The concept only accounts for thermal annealing, any irradiation effects such as gamma annealing are not accounted for
2. The concept was developed when only low fluence data were available
3. The reasoning behind the concept assumes that a higher temperature always reduces damage to the crystallite and hence the polycrystalline structure. Using dimensional change as a yardstick of damage it can be seen that, before turnaround, between about 300°C and 600°C there may be some substance to the concept, but after turnaround, this is clearly not the case
4. For temperatures above 900 °C the reasoning appears to break down altogether.

The current position at PBMR, is to ignore the concept of equivalent temperature until such time as better high temperature, high fluence data become available. This makes interpretation of Materials Test Reactor, MTR data from different reactors difficult and increases the uncertainty in the assumed graphite irradiated material properties for PBMR.

#### PBMR Irradiated Material Database

Currently there are no materials available from any manufacturer that have an irradiation database that covers the irradiation requirements of the PBMR to achieve a 35 fpy life. The SGL materials above will be based on sleeve graphites currently used in the UK AGR programme. However, due to the larger block sizes identical material cannot be guaranteed by the manufacturer. The properties of the sleeves have recently changed due to the lack of availability of vft coke. The manufacturer identified a suitable alternative coke from NSCC. Therefore some low fluence, low temperature data exists for a similar material.

Additionally, from the various government sponsored programmes in the 1950's and 1960's there is a considerable body of data on the irradiated properties of graphite and several semi-

empirical relationships have been developed to describe the irradiation induced material property changes of graphite. This body of data best describes graphite irradiation at low fluences, up to the point of turnaround, and this can be used to generate a PBMR graphite database for use in graphite performance assessments.

The PBMR irradiated graphite database has been based, firstly, on an interpretation of the “family” characteristics of two graphites, ATR-2E and VQMB and, secondly, on the irradiation theory of graphite crystals described above.

It is assumed that for the type of graphite to be used in PBMR, in the temperature and fluence range of interest, the graphite behaviour is consistent, i.e. the material properties, when irradiated in a similar flux, may be described by mathematical equations, which are a function of irradiation temperature and dose.

### Dimensional Change

Mrozowski suggested that when a graphite cools from the graphitisation temperature, during manufacture, cracks are formed within the crystallite due to the large difference in  $\alpha_a$  and  $\alpha_c$ . At low fluence these cracks are able to accommodate c-axis growth and the net effect is shrinkage. At higher fluences, beyond turnaround these cracks have all closed and the c-axis growth leads to significant straining of the crystallites.

At all temperatures of interest in the PBMR, both graphites shrink both parallel and perpendicular to the grain before “turning around” and swelling until the original volume is attained and beyond. The key points that the PBMR dimensional change curves are based on are:

- The dose where the dimensional change curve crosses back over the zero growth axis.
- The dose where the dimensional change curve reaches maximum shrinkage.
- The value of dimensional change at the point of maximum shrinkage.

### CTE

Up to the point of ‘turnaround’ the irradiated behaviour of the CTE can be described through a relationship with dimensional change. Therefore the CTE behaviour can be derived from the dimensional change curves.

Beyond turnaround the relationship breaks down and the PBMR database relies on scant data from ATR-2E and VQMB. At various temperatures some extrapolation in fluence has been necessary due to paucity of data.

### Thermal Conductivity

Though this section deals with thermal conductivity (K), it is usual in graphite technology to work in thermal resistance (1/K). As previously discussed, heat is conducted much more easily along the basal plane than perpendicular to it. In the range of interest for the PBMR thermal resistance in graphite increases with increased temperature. Irradiation further

increases the thermal resistance and in addition alters the temperature dependence of the thermal resistance.

Much of the thermal resistance data for irradiated graphite are measured at room temperature, therefore a methodology is required to calculate the thermal resistance of graphite at various reactor operating temperatures and irradiation doses.

The thermal resistance of a polycrystalline graphite in some arbitrary direction 'y' (usually defined as one of the extrusion directions) as a function of dose and temperature and referred back to the unirradiated value can be given as:

$$\frac{1}{K_y(\gamma, T)} = \frac{1}{K_y(0, T)} + \frac{1}{K_i(\gamma, T)}$$

Where T is the real temperature and  $\gamma$  is the dose.

Based on UK methodology the parameter  $1/K_i(\gamma, T)$  has been shown to be separable into two parts, firstly, the change in thermal conductivity due to irradiation (measured at 30°C),  $f$ , and, secondly, the temperature dependency of the change in thermal conductivity due to irradiation,  $\delta(T)$ . This leads to the relationship for the thermal resistivity in polycrystalline graphite of:

$$\frac{1}{K_y(\gamma, T)} = S_k(\gamma) \left[ \frac{1}{K_y(0, T)} + \delta(T) \frac{f}{K(0, 30)} \right] \left[ \frac{K_o}{K} \right]_{ox}$$

Where

$$f = \frac{K_y(0, 30)}{K_y(\gamma, 30)} - 1$$

Is the ratio of the unirradiated change in thermal conductivity measured at 30°C to the change in thermal conductivity at the required damage, also measured at 30°C and

$$\delta(T) = \frac{\frac{1}{K_i(\gamma, T)}}{\frac{1}{K_y(\gamma, 30)}}$$

Is the temperature dependent thermal resistance after irradiation.

The structural factor  $S_k(\gamma)$  is applicable at high Fluences. The term  $[K_o/K]_{ox}$  is an oxidation factor derived from irradiations in Carbon Dioxide. For the PBMR and irradiation in helium this term can be assumed to equal 1.

Therefore to predict the change in thermal conductivity due to fast neutron irradiation, data are required for the unirradiated temperature dependence of thermal conductivity,

$K_y(0,T)/K_y(0,30)$ , the change in thermal resistance measured at room temperature as a function of dose and temperature,  $f$ , the temperature dependence of the irradiation induced change to thermal conductivity,  $\delta(T)$  and the structural factor to account for high fluence (beyond 'turnaround' behaviour).

### Young's Modulus

Young's modulus is measured either by carrying out a static test (tension, compression or bend) or by measuring the dynamic (resonant) modulus. As the stress-strain curve of unirradiated graphite is non-linear and exhibits hysteresis, its value will depend on the number of the cycle at which the measurement was taken and value of strain used in the measurement.

The stress-strain behaviour of polycrystalline graphites is highly non-linear, both in tension and compression, with the stress to strain relationship increasing with increasing cyclic stress. The elastic modulus of graphite increases with temperature up to  $\sim 2000^\circ\text{C}$  before decreasing to zero at  $\sim 3000^\circ\text{C}$ . However, over the temperature range of interest in the PBMR, the increase is considered to be insignificant.

As previously discussed, irradiation significantly increases the shear modulus parallel to the basal plane of the crystallite ( $C_{44}$ ) due to pinning of the glissile dislocations. This is reflected in significant irradiation stiffening at low doses.

At the temperatures of interest in the PBMR, after this initial irradiation stiffening, the modulus increases. This is attributed to a decrease in the porosity, due to crystallite deformations. Eventually the modulus stops increasing and starts to decrease due to the generation of new porosity. This continues until the graphite returns to its original volume and starts to disintegrate.

Both VQMB and ATR-2E show little differences in irradiation induced modulus changes in the two principal directions.

### Poisson's Ratio

There is some evidence that Poisson's ratio changes with irradiation, however data are very sparse. It is therefore recommended that a typical Poisson's ratio of 0.2 is used for PBMR graphite and is assumed to be independent of material direction and irradiation.

### Irradiation Induced Creep

Thermal creep in graphite is very small and is usually quoted as being insignificant below  $1800^\circ\text{C}$ . However when graphite is irradiated by fast neutrons it creeps at temperatures much lower than would be the case without the presence of irradiation.

Irradiation creep experiments are difficult and expensive to carry out. For this reason there is an extensive irradiation creep database at low doses and intermediate temperatures, but not as much information at high temperatures and intermediate and high Fluences.

With increasing fluence there is an initial period of primary creep strain, which appears to be recoverable on load removal, followed by a linear increase in creep strain. At intermediate dose levels the creep strain rate reduces, but at high doses it increases again. Much larger

strains can be tolerated with irradiation creep than would be the case for pure elastic loading. In the UK, an irradiation creep strain of 2% is often quoted as the limiting creep strain, although higher values of creep strain have been recorded.

In the UK, the study of irradiation creep came into prominence when the case for the CAGR was being made. Various graphites were irradiated in creep experiments. In the UK, irradiation creep strain in graphite is usually described for both positive (tensile) and negative (compressive) creep by a simple linear visco-elastic model that includes a primary and secondary creep term:

$$\varepsilon_c = \alpha(T_i) \frac{\sigma}{E_c} \left[ 1 - e^{-\frac{\gamma}{\gamma_0}} \right] + \frac{K}{E_c} \beta(T_i) \sigma \gamma$$

Where  $\sigma$  is the applied stress,  $E_c$  is the creep modulus,  $\gamma$  is the neutron dose scale,  $\alpha(T_i)$  and  $\beta(T_i)$  are irradiation temperature and dose dependent factors and  $K$  and  $\gamma_0$  are constants.

The creep modulus accounts for the reduction in creep rate at intermediate irradiation doses and the rapid acceleration in creep rate at higher doses. The creep modulus is defined as  $E_s$ . Where  $E_s$  is the modulus structure term defined by the relationship:

$$\left[ \frac{E}{E_0} \right]_s = \left[ \frac{E}{E_0} \right] / \left[ \frac{E}{E_0} \right]_p$$

Where  $[E/E_0]_p$  is the pinning term for modulus.

The reasoning behind this definition of creep modulus is that creep strain has been shown to be inversely proportional to the aggregate modulus and proportional to the crystal shear modulus. Pinning modifies the aggregate modulus through the crystal shear modulus, thus changes to the moduli cancel each other out.

The primary creep is considered to be recoverable and equal to one elastic deflection. It is often ignored in assessments, however, the magnitude of primary creep at high temperatures may be larger as discussed below.

In the PBMR temperature range both  $\alpha(T_i)$  and  $\beta(T_i)$  are a function of temperature, see Table below, although there is some uncertainty in the value of  $\alpha(T_i)$ . This temperature dependent increase in secondary creep coefficient is also confirmed by the Russian and US creep laws.

### Creep rate temperature dependence

$T_i$ (°C)	$\alpha(T_i)$	$\beta(T_i)$ *
300-650	1	1.0
850	1	1.5
1050	3.5	1.5

\* assuming  $K=0.23$

The above describes the UK creep model and, as usual in graphite technology, there is not unanimous support for this model. An alternative creep model has been proposed based on

volumetric dimensional change to improve predictions at high fluence. This will be investigated by PBMR.

### Component Performance Assessment

Graphite is a brittle material and the failure strength depends on component size, geometry and mode of loading. For specimens of a similar size, graphite is stronger in compression than bending and stronger in bending than tension. Thus, it is difficult to predict the failure of a graphite component from small specimen tests even without considering the complexity of irradiation damage.

In practice, as graphite is a brittle material, the failure criteria are compared with the maximum principal stress, as von Mises or other similar criteria as applied to metals would not be appropriate.

In the UK, it has been the practice to carry out failure tests on full size components in all of the predicted loading modes. These tests, along with finite element assessments are then used to predict the failure stress at the critical load. As failure is a statistical process, it is necessary to carry out enough tests to determine the mean and standard deviation for use in probabilistic assessments. Having obtained these data for the unirradiated components, the failure stresses are then modified for the effect of fast neutron irradiation and thermal or radiolytic oxidation using the methods described below.

In Japan, a criteria for the design of HTTR components was developed based on a modified version of ASME code, see below. The code uses a minimum ultimate tensile strength determined from a statistical analysis of unirradiated strength data with a survival probability of 99% at a confidence level of 95%. This statistical assessment was based on a normal distribution fitted to about 260 tensile tests. The component stresses are then resolved into primary plus secondary (membrane, membrane plus bending) and peak stress (peak, fatigue). These stress components can then be compared with the minimum ultimate tensile stress scaled by a safety factor depending on the operating conditions and the type of component.

### **DESIGN STRESS LIMITS FOR CORE SUPPORT GRAPHITE COMPONENTS AND CORE GRAPHITE COMPONENTS - JAERI**

OPERATION CONDITION CATEGORY	PRIMARY PLUS SECONDARY STRESSES		PEAK STRESS	
	MEMBRANE $P_m, Q_m$	MEMBRANE PLUS BENDING OR POINT $P_b, Q_b, P_p, Q_p$	PEAK $F$	FATIGUE
I & II	$P_m + Q_m$	$P_m + Q_m + P_b + Q_b$ OR $P_p + Q_p$	$P_m + Q_m + P_b + Q_b + F$ OR $P_p + Q_p + F$	$1/3$ <sup>2)</sup>  $2/3$  $3/3$
III	$0.25 Su$ <sup>1)</sup>	$0.33 Su$	$0.9 Su$	
IV	$0.5 Su$	$0.67 Su$	$0.9 Su$	
	$0.6 Su$	$0.8 Su$	$1.0 Su$	

- 1)  $S_u$  is the specified minimum ultimate strength of the material.
- 2) Allowable fatigue life usage fraction

The US have also proposed an approach linked to the ASME code (although the details have not yet been obtained by PBMR) and includes a modified Weibull distribution and a probability of crack initiation of  $10^{-4}$ .

In Germany it is proposed that the Weibull distribution can be used to determine a factor of safety that can be readily used for design purposes. An allowable stress has been defined as the mean strength  $\bar{\sigma}$  divided by a safety factor  $S$ :

$$\sigma_{\text{allowed}} = \frac{\bar{\sigma}}{S}$$

Applying a two parameter Weibull relationship for a uniaxial stress state the factor of safety can be defined in terms of a failure probability,  $F$  and the Weibull modulus 'm'. The Weibull modulus defines the scatter of the data, the higher the modulus the less the scatter in the data.

The table below was derived using this method.

### Safety Factor $S$ for failure probabilities $F$

m	S for				
	$F=10^{-2}$	$F=10^{-3}$	$F=10^{-4}$	$F=10^{-5}$	$F=10^{-6}$
2	8.8	28.0	88.6	280.3	2802.5
5	2.3	3.7	4.6	9.2	23.1
10	1.5	1.9	2.4	3.0	4.8
15	1.3	1.5	1.8	2.1	2.8
20	1.2	1.4	1.5	1.7	2.2
30	1.1	1.2	1.3	1.4	1.7

In Germany, the allowed failure probability for graphite components whose failure would cause severe damage, or represents a risk for the further operation of the reactor, is  $10^{-4}$ . In this case, the allowable stress is the corresponding strength divided by a factor of about 2.5.

However there is little data to determine the effect of irradiation on Weibull parameters. The Table below shows the data used in the PBMR database.

## Variation of Statistical Distributions for Failure Stress

	Parallel			Perpendicular		
	m	$\sigma_o$ (Mpa)	Number of samples	m	$\sigma_o$ (Mpa)	Number of samples
Unirradiated	7.4	13.1	61	8.6	9.4	59
425-465 °C	9.2	25.6	8	4.5	17.1	8
605-785 °C	6.6	22.8	21	5.9	18.0	23
845-1005 °C	5.9	20.1	33	4.1	15.7	36

The number of samples in the 425-465°C-temperature range is too small to give reliable statistics. Therefore, these data should be ignored. However, the results do indicate a reduction in Weibull modulus with irradiation as a function of irradiation temperature and dose and hence an increase in the scatter.

Fast neutron irradiation rapidly increases the strength due to pinning of the dislocations in the basal planes. Following this initial hardening, there is a further increase in strength with increasing dose, due to structural effects, until a peak is reached after which the strength decreases due to the generation of porosity.

The UK proposed that Griffith failure criteria should be applied to graphite and that failure would occur at constant strain energy to failure per unit volume. Thus, the strength of irradiated graphite could be equated to the strength of unirradiated graphite by:

$$\frac{1}{2} \frac{\sigma_o^2}{E_o} = \frac{1}{2} \frac{\sigma^2}{E}$$

where  $E_o$  and  $\sigma_o$  are the unirradiated modulus and strength and  $E$  and  $\sigma$  are the irradiated modulus and strength. This led to the well-used relationship:

$$\frac{\sigma}{\sigma_o} = \left( \frac{E}{E_o} \right)^n$$

Where 'n' is usually taken as 0.5.

By experimentation on various graphites, for the irradiation temperatures between 300°C and 500°, the square root relationship has been shown to hold true. However, at very high irradiation doses and temperatures of interest to the PBMR the relationship may break down and 'n' is considered to approach unity. Unfortunately, there are little data in this range. In safety and lifetime prediction assessments carried out in the UK the square root rule is used up to the peak in the modulus change versus dose curve. After this 'n' is taken to be unity. This has been adopted by PBMR.

Based on the discussion given above the recommended failure criteria for PBMR graphite components is:

- a) Maximum principal stresses should be used.
- b) A factor of safety of 1.5 should be used applied to the mean failure stresses in tension or compression. In the case of local bending or local tension, a factor of 1.0 on the tensile strength should be used. For high-risk components, a factor of 2.5 is recommended. The stresses should be modified using a power law with  $n = 0.5$  or 1 depending on the change in modulus as described above.

### **Performance Assessment Criteria**

Due to a combination of differential thermal strains and differential irradiation induced dimensional change strains complex strain distributions develop during the lifetime of PBMR graphite reflector components. This internally generated load has to be combined with several other loads such as, pebble bed silo load, differential coolant pressure, component deadweight, seismic, flow induced vibration and acoustic vibration generated by significant gas speeds.

For best estimate calculations PBMR has adopted the German approach to performance evaluation and employed a probability of failure of  $10^{-4}$  for safety critical components. Finite element codes such as Marc or ABAQUS will be used to model the linear visco-elastic behaviour in specially written material models. These models will be validated against other codes developed in the US, UK or Germany. The early indications are that 35 fpy will be difficult to substantiate in part of the side reflector using best estimate calculations.

PBMR will most likely adopt the UK approach to probabilistic assessment of graphite component performance. This basically involves assembling all influencing factors, carrying out sensitivity studies to determine the most important factors, assigning distributions to those factors, using sampling techniques to reduce the number of analyses required and several hundred finite element analyses to determine the probability of failure. A probability of failure of  $10^{-4}$  has been set for all safety critical components. This is in line with German and US approaches. A lower probability of failure may be assigned for other components such as side reflector blocks as the sleeve is the safety critical component.

Deformation is mainly strain induced (thermal, irradiation & creep) and could lead to lack of insertion of RCSS, excessive bypass flows and failure of components due to interaction with neighbours. Control rod articulation within the graphite sleeves of the side reflector will determine the allowable deformation associated with sleeve bowing and sleeve ovaling. However the sleeves are designed to be replaceable (to cater for a dropped control rod event).

Structural Performance and Deformation are a function of design and reactor parameters. Material exhaustion is a function of reactor parameters only i.e. the fluence and irradiation temperature will pre determine the material exhaustion limit.

Material exhaustion is the point at which the graphite structure is basically disintegrating due to the damage to caused by the neutron fluence. Some parts of the PBMR @ 35 fpy will see a peak fluence of  $\sim 165 \cdot 10^{20} \text{ n/cm}^2$  or  $\sim 20 \text{ dpa}$  at approximately 750 deg C. This means that on

the front face of the side reflector every atom will have been displaced from its lattice position 20 times during the course of the operation of the plant.

## Risk Mitigation

Faced with the prospect of uncertain graphite data beyond turnaround and uncertain performance predictions, PBMR decided that two additional pieces of work were required in order to achieve the desired graphite performance. These consist of an MTR programme and an investigation into feasibility of replacing the inner graphite reflector.

### MTR Programme

The nuclear industry worldwide has generated a significant amount of data on a number of graphites over the last three or four decades. This data has developed into an advanced body of knowledge concerning the behaviour of graphite when subjected to irradiation. However lack of detailed knowledge of the particular graphite under consideration still leads to uncertainty in the prediction of graphite behaviour beyond turnaround. This is due to a combination of the inherent uncertainty in graphite properties and the difficulty associated with extrapolation of data from one particular graphite to another. This problem is accentuated for PBMR where lifetime fluence requirements are onerous for some of the operational temperatures. Therefore in order to adequately assess the performance of PBMR graphite components subjected to high fluence, a comprehensive irradiation programme is required.

PBMR wish to irradiate the specimens at two or three fixed temperatures in the range 500 to 950°C. Equal numbers of specimens will be irradiated at the two or three temperatures.

The temperature of the specimens must be continually monitored by thermocouples embedded in the carrier at various axial positions and the correlation between the actual specimen temperature and the thermocouple-measured temperature must be demonstrated by experiment or calculation.

The Table below indicates the number and extent of samples to be examined during the course of the irradiation. It has been assumed that the same specimens can be used for all non destructive tests, except the creep strain measurement and one of the destructive tests at each fluence required thereby minimising the total number of specimens.

Fluence	$\epsilon$	$\epsilon_c$	$\rho$	CTE (20-120)	K (20)	E (20)	CTE (20-1200)	K (20-1200)	$\alpha_c$ (20)	$\sigma_T$ (20)	$K_\gamma$
0	6	12*	6	6	6	6	6	6	6	6	6
1	6	12	6	6	6	6	6	6	6	6	6
2	6	12	6	6	6	6	6	6	6	6	6
3	6	12	6	6	6	6	6	6	6	6	6
4	6	12	6	6	6	6	6	6	6	6	6
5	6	12	6	6	6	6	6	6	6	6	6
6	6	12	6	6	6	6	6	6	6	6	6

For creep experiment 6 tensile creep and 6 compressive creep specimens will be required. Young's modulus and Poisson's ratio can be measured on the  $\sigma_t$  specimens.

Total number of specimens is the summation of these specimens – assumes that all non-destructive tests, except creep strain could be performed on one or more sets of specimens prior to final destructive test. One set of six specimens will be used for all creep strain measurements. Total number of irradiation Specimens is 186 per material per irradiation temperature. Minimum of 3 irradiation temperatures is required.

As discussed earlier there is considerable debate within the graphite community on the effect on damage in graphite due to the rate at which the damage is accumulated. There are a couple of basic options to PBMR – irradiate the small samples in a high flux reactor ( a factor of ~ 40 times the flux in PBMR) and obtain results in 12 to 14 months or irradiate small samples in a lower flux reactor (approximately 4-6 times the PBMR flux) and obtain results in 8 to 10 years. It is hoped that these difficulties will be resolved however PBMR is of the opinion that there is sufficient data to justify graphite performance for at least 15 fpy and therefore believes that either option will be suitable.

### Inner Reflector Replacement System

A host of reflector replacement options were studied ranging from complete core barrel change to limited reflector replacement. At present the favoured solution is replacement of the inner reflector through the central plug in the top reflector. This solution minimises disruption to the core structures and the associated interfaces to the RCSS, FHSS, and CCS etc. As a result it also offers the potential of the fastest time to change the reflector.

The side reflector is arranged in two columns and the inner column has a thickness of 400mm. Thus the irradiation-induced damage to the outer permanent reflector is small. The bottom cone blocks are also limited in life due to severe temperature gradients caused by the graphite sphere central column and severe fluence gradients in the reflector. These blocks will also be replaced part way through life. The bottom reflector blocks will be replaced to a depth where the irradiation-induced damage will be small.

The replacement strategy would mitigate risk from lifetime issues

- Structural Performance
- Distortion
- Material Exhaustion

The replacement strategy would also increase the margin to the peak fuel temperature limit under normal and abnormal conditions, as the high fluence effect on thermal conductivity would not have materialised at time of replacement.

### Conclusions

1. There is substantial experience in operating gas-cooled, graphite moderated reactors around the world, e.g. UK.
2. Suitable Nuclear Grade Graphites can be determined by appropriate choice of manufacturing process parameters

3. Sufficient information is available to justify PBMR operation up to the point of turnaround, approximately 15 full power years at the peak flux position.
4. Graphite Technology is still mainly empirical, especially at high fluence and temperature and uncertainty exists in the material database assumed for PBMR beyond turnaround
5. A MTR programme is required to characterise PBMR graphite and to remove uncertainty associated with performance assessment of PBMR graphite components beyond turnaround
6. The risks associated with performance of graphite components in PBMR can be mitigated by replacement of the inner reflector